# Optimization of a Flyback Transformer Winding Considering Two-Dimensional Field Effects, Cost and Loss

C. R. Sullivan
T. Abdallah
T. Fujiwara

Found in *IEEE Applied Power Electronics Conference,* Mar. 2001, pp. 142–150.

# Optimization of a flyback transformer winding considering two-dimensional field effects, cost and loss

Charles R. Sullivan, Tarek Abdallah
Dartmouth College, Hanover, NH, USA, http://engineering.dartmouth.edu/inductor
Toru Fujiwara
Matsushita Electric Works, Osaka, Japan

*Abstract*—**The largest loss in an example litz-wire flyback transformer is found during current commutation between windings. In order to reduce this loss, a new optimization method is introduced. The new method optimizes strand size and number in litz wire considering cost and loss. Unlike previous methods, it is valid with two- or three-dimensional field geometry and with different non-sinusoidal waveforms in any number of windings. The result of applying this method to the example flyback transformer is less expensive designs with lower loss, as confirmed by experimental measurements.**

## I. Introduction

DESIGN of high-performance magnetic components for high-frequency power converters poses many challenges. In particular, winding losses at high frequency can drastically degrade performance. Some of the issues addressed by recent work on high-frequency windings include non-sinusoidal currents [1], [2], [3], [4], [5]; the effect of gaps and the resulting two-dimensional fields [6], [7], [8], [9], [10], [4]; modeling of losses in litz wire [3]; tradeoffs between cost and loss [11], [12]; and mutual-resistance effects[1] [13], [4].

Flyback transformers entail particularly interesting magnetics design [14], [15], because all of these issues become important simultaneously, particularly if the transformer is wound with litz wire and is intended to be produced at low cost. The waveforms are far from sinusoidal, and they differ in both form and phase between different windings, making mutual resistance[1] an important effect. A gapped ferrite core is usually used, and the gap produces a two-dimensional field, the effect of which must be evaluated and perhaps mitigated. And both the cost and the loss in the litz-wire winding are strong functions of the diameter and number of strands chosen, making the choice of these parameters critical to both performance and cost.

In this paper, we address just such a case: a flyback transformer wound with litz wire. The application and the original design of the transformer are listed in Table I. We undertook to improve the design of the winding to reduce loss in the transformer, taking cost into consideration. The first step was to evaluate loss in the original design and consider possible strategies to improve it (Section II). As a result of this analysis, we chose to investigate optimizing the litz-wire stranding in the winding as the most promising initial step toward improving the design. Thus in Section III, we study the optimization of cost and loss in a litz-wire transformer winding, similar to the analysis in [11], [12]. However, our new analysis can be applied to more general situations than can that in [11], [12], including the two-dimensional fields and different non-sinusoidal currents in each winding that we are faced with in this design. The resulting new designs have been tested in the flyback converter and the results confirm the validity and utility of the new technique.

[1] Although high-frequency winding losses are often modeled by ac resistance, ac resistance has no direct physical meaning and is only a way of normalizing winding loss to winding current. The ac loss occurring in any given winding depends more directly on the field impinging on that winding than on the current flowing in it. The field can result from a combination of currents in different windings, and depending on their relative phase the resulting field magnitudes may add or cancel. Thus the losses depend on the phase relationships between different winding currents. The loss characteristics may be correctly described by a resistance matrix, including self- and mutual-resistances, which may be frequency dependent [13]. For many transformers, the same effects may accounted for in a frequency-independent matrix by using the squared-field-derivative (SFD) method [4].

## II. Evaluation of Original Design

The squared-field-derivative (SFD) method [16], [4] was chosen to evaluate the loss in the existing design because it accounts for disparate non-sinusoidal waveforms, includes mutual-resistance effects, and, unlike direct use of finite-element analysis to calculate eddy-current loss effects, it allows treating litz-wire windings accurately without great computational expense. The method uses a set of simplified magnetostatic finite-element simulations to obtain parameters for a "dynamic loss matrix", $\mathbf{D}$, which describes the transformer. This matrix can then be used to calculate loss with any set of waveforms from the expression

$$P_e = \overline{\begin{bmatrix} \frac{di_1}{dt} & \frac{di_2}{dt} \end{bmatrix} \mathbf{D} \begin{bmatrix} \frac{di_1}{dt} \\ \frac{di_2}{dt} \end{bmatrix}} \qquad (1)$$

where $P_e$ is the total time-average eddy-current loss in both windings, and $\overline{\cdot}$ indicates a time average.

For this design, we first found the value of $\mathbf{D}$ according to the method in [4] as listed in Table II. Then, with idealized triangular current waveforms, we can calculate loss for each time period, as is also shown in Table II. The idealized triangular current waveforms used in the calculation neglect any ringing near the transitions. As will discussed in Section IV, it

TABLE I

CONVERTER SPECIFICATIONS AND INITIAL TRANSFORMER DESIGN

| Converter Specifications | |
|---|---|
| Topology and Mode | Discontinuous Flyback |
| Input | 14 V |
| Output | 85 V, 0.4 A |
| Switching Frequency | 130 kHz |

| Initial Transformer Design | |
|---|---|
| Primary Winding | 7 turns, 100 strand litz (50x2); 0.1 mm strand diameter |
| Secondary Winding | 49 turns, 28 strand litz; 0.1 mm strand diameter |
| Core | Geometry: LP 27/13; Material: TDK PC44 MnZn Ferrite |
| Gap | 1 mm |

TABLE II

LOSS CALCULATION IN ORIGINAL DESIGN USING SFD METHOD

$$\mathbf{D} = \begin{bmatrix} 3.42 & 0.329 \\ 0.329 & 0.043 \end{bmatrix} \times 10^{-13}\ \Omega\mathrm{s}^2$$

| Time period: | Primary ramp up | Transition to secondary | Secondary ramp down |
|---|---|---|---|
| Eddy loss: | 0.019 W | 0.447 W | 0.030 W |

| Winding | DC resistance | RMS current |
|---|---|---|
| Primary | 6 mΩ | 4.65 A |
| Secondary | 200 mΩ | 0.67 A |

| Total resistive loss ($\sum I_{rms}^2 R_{dc}$) | Total eddy loss (1) | Total winding loss |
|---|---|---|
| 0.22 W | 0.50 W | 0.72 W |

is best to consider ringing losses separately from the loss due to the ideal waveforms, considered here.

The loss breakdown by time period in Table II can be useful for evaluating possible approaches to improving the design. One approach would be to consider the effect of the gap and its fringing field on the winding loss [15] and to consider changes in the design such as a distributed or quasi-distributed gap [7] or an optimized winding shape [9], [10]. However, from Table II, we see that the bulk of the loss occurs during the transition between the two windings, during which the field in the gap is not changing significantly (Fig. 1). Thus, loss due to the field of the gap is contained almost exclusively in the first and last time periods, and it constitutes less than 10% of the eddy current loss; the loss during the transition is of much greater importance [14]. Thus, the first priority for improving the transformer is to decrease the ac loss associated with this transition. Note that the converter considered here operates in discontinuous mode, which means that the field in the gap varies more than it would in a lower-ripple continuous-conduction converter. Therefore, there are higher losses associated with the gap field in this case than there are in many others, but even in this "worst-case" situation, the gap losses are still small compared to the transition losses.

Possible strategies for reducing loss during the transition include interleaving of primary and secondary windings, or changing the number and size of strands in the litz winding. Interleaving would affect leakage inductance as well as ac winding loss. Reduced leakage inductance would reduce switching losses in the circuit, and would shorten the transition time. From (1), we can see that the resulting large values of $di/dt$ could increase winding loss at the same time that they reduce circuit loss. But a prerequisite to careful consideration of the tradeoffs between winding loss in the transformer and switching loss in the circuit is a careful optimization of winding design, holding the circuit operation fixed. Thus, in this paper, we look carefully at what improvements are possible in the transformer without affecting circuit operation; keeping leakage inductance, and thus both switching losses and current transition slope, constant.

In the following sections, we analyze the choice of strand size and number in the litz-wire windings. As shown in [11], [12], the stranding that minimizes loss is usually prohibitively expensive, and often requires finer wire than is commercially available. Thus, for an analysis to be of practical use to a designer, it must also consider cost. However, the analysis in [11], [12] cannot be directly applied, because it assumes a one-dimensional field geometry and because it assumes equal currents in the two windings. Thus we need to find a way

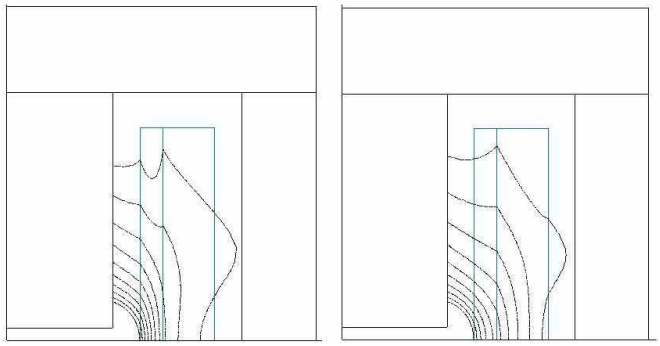

Fig. 1. Field strength in a quarter-cross section of the flyback transformer. The rectangles are the two windings (center) and the core (left, top and right) with the gapped centerpost at the left. Plotted are contour lines of field strength from magnetostatic finite-element analysis. The left plot is for current only in the primary (inner winding) just before the switch turns off in the flyback converter, and the right plot is for current only in the secondary (after the primary switches off). The plotted lines are not field lines or equipotential lines, but are contour lines of equal field strength, spaced by 4 kA/m, ranging from 4 to 40 kA/m. Higher fields are present in the gap region but the 40 kA/m range is chosen for plotting in order to show the effects in the winding region. By comparing the two plots, one can see that the field in the region near the gap does not change significantly, but the field between the windings does change. Because the field near the gap changes only much more slowly, the fringing-field contribution to eddy current losses is small. This was determined quantitatively from the data in Table I, as discussed in the text; these plots are included only as illustrations, not as evidence of the relative magnitudes of different loss effects.

to extend the analysis in [11], [12] to more general situations such as those addressed by the SFD method [4].

## III. Design Analysis

The analysis of litz cost and loss in [11], [12] is based on the ac resistance factor, $F_r = R_{ac}/R_{dc}$, which can, for the simple configurations addressed in [11], [12], be expressed:

$$F_r = 1 + \frac{k\pi^2\omega^2\mu_0^2 N^2 n^2 d_c^6}{768\rho_c^2 b_c^2} \tag{2}$$

where $\omega$ is the radian frequency of a sinusoidal current, $n$ is the number of litz-wire strands, $N$ is the number of turns, $d_c$ is the diameter of the conductor in each strand, $\rho_c$ is the resistivity of the conductor, $b_c$ is the breadth of the window area of the core, and $k$ is a factor accounting for field distribution in multi-winding transformers [17], [3]. To apply a similar approach to more general situations, we introduce a factor $F_e$, analogous to $F_r$, but defined as the ratio of the actual losses to the losses expected based on dc resistance:

$$F_{e,j} = \frac{P_{w,j}}{P_{r,j}} = 1 + \frac{P_{e,j}}{P_{r,j}} \tag{3}$$

where $P_w$ is the total power lost in the winding, $P_e$ is the power lost due to eddy currents, $P_r$ is the loss expected based on dc resistance ($P_r = I_{rms}^2 R_{dc}$), and the subscript $j$ indicates quantities for winding $j$ in a multi-winding transformer. Without dc current or mutual resistance effects, $F_e$ and $F_r$ are equal; (2) is also an expression for $F_e$ in the simple situations analyzed in [11], [12]. We can rewrite (2) in terms of the cross-sectional area of a strand ($A_{s,j} = d_{c,j}^2 \frac{\pi}{4}$), as

$$F_{e,j} = 1 + k_\ell n_j^2 A_{s,j}^3 \tag{4}$$

where $k_\ell$ represents constant terms of (2) lumped together. If $F_e$ can, for some other situation, be expressed in a form identical to (4), the analysis in [11], [12] can be applied to optimize cost and loss.

We observe that the analysis in [4] shows that the power loss due to eddy currents in any winding, $P_e$, varies with $nA_s^2$ and that the resistive power loss depends on the dc resistance and is proportional to $(nA_s)^{-1}$. And since $F_e$ varies directly with $P_e$ and inversely with $P_r$ as in (3), we have

$$F_{e,j} = 1 + \frac{k_1 n_j A_{s,j}^2}{\frac{k_2}{n_j A_{s,j}}} \tag{5}$$

where $k_1$ and $k_2$ are constants relating power losses to their respective $n$ and $A_s$ terms. After simplification, (5) yields (4) with $k_\ell = k_1/k_2$. This shows that the more general situation analyzed in [4] yields an expression for loss of the form (4) and, consequently, the procedure in [11], [12] can be used to optimize cost and loss. However, in order to implement the optimization in [11], [12], a value for $k_\ell$ must be calculated.

To find $k_\ell$, we equate (4) and (3); solving for $k_\ell$ yields

$$k_\ell = \frac{P_{e,j}}{P_{r,j} n_j^2 A_{s,j}^3} \tag{6}$$

This expression could be used to calculate $k_\ell$ from a completed design to evaluate loss in that design. Note that while $k_\ell$ is expressed in terms of $n$ and $A_s$ in (6), it does not vary with these quantities, due to the dependence of $P_e$ and $P_r$ upon them. Knowing $k_\ell$ at the beginning of the analysis prior to calculating values for $n$ and $A_s$ is often convenient when seeking an optimal design. A procedure, based on [4], for calculating $k_\ell$ without $n$ and $A_s$ is derived in the following section.

### A. Evaluation of $k_\ell$

Reference [4] defines a loss coefficient, $\gamma_j$ for each winding $j$, dependent on the winding parameters. A modified loss coefficient may be defined as

$$\tilde{\gamma}_j = \frac{\gamma_j}{n_j A_{s,j}^2} = \frac{N_j \ell_{w,j}}{4\pi\rho_c}. \tag{7}$$

Here, $\ell_w = N\ell_t$ and is the length of the entire winding. As shown in [4], $P_e$ can be found by establishing a dynamic resistance matrix, $\mathbf{D}$, containing transformer characteristics. In the pursuit of finding $k_\ell$ independent of $n$ and $A_s$, we define a

modified dynamic resistance matrix $\tilde{\mathbf{D}} = \frac{\mathbf{D}}{\mathbf{n_j A_{s,j}^2}}$:

$$\tilde{\mathbf{D}} = \tilde{\gamma}_1 < \begin{bmatrix} \left|\hat{\vec{B}}_1\right|^2 & \hat{\vec{B}}_1 \cdot \hat{\vec{B}}_2 \\ \hat{\vec{B}}_2 \cdot \hat{\vec{B}}_1 & \left|\hat{\vec{B}}_2\right|^2 \end{bmatrix} >_1 + \tilde{\gamma}_2 < \begin{bmatrix} \left|\hat{\vec{B}}_1\right|^2 & \hat{\vec{B}}_1 \cdot \hat{\vec{B}}_2 \\ \hat{\vec{B}}_2 \cdot \hat{\vec{B}}_1 & \left|\hat{\vec{B}}_2\right|^2 \end{bmatrix} >_2 = \sum_j \tilde{\mathbf{D}}_j \quad (8)$$

where $\hat{B}_j$ is the magnitude of the field everywhere arising from the current in winding $j$ and $<>_j$ signifies the spatial average over the region of the winding $j$. In [4], the sum of the winding terms is used to calculate total loss; we now need to find the losses in individual windings in order to optimize their stranding parameters ($n_j$ and $A_{s,j}$), so we have defined the corresponding individual terms, $\tilde{\mathbf{D}}_j$. The eddy current loss can be related to the modified dynamic resistance matrix:

$$P_{e,j} = n_j A_{s,j}^2 \overline{\left[\begin{array}{cc} \frac{di_1}{dt} & \frac{di_2}{dt} \end{array}\right] \tilde{\mathbf{D}}_j \left[\begin{array}{c} \frac{di_1}{dt} \\ \frac{di_2}{dt} \end{array}\right]}. \quad (9)$$

The resistive loss can be written

$$P_{r,j} = I_{rms,j}^2 R_{dc,j} = \frac{I_{rms,j}^2 \ell_{w,j} \rho_c}{n_j A_{s,j}}. \quad (10)$$

Now it is possible to obtain $k_\ell$ using (6) and, as a consequence, show the independence of $k_\ell$ with respect to the number of strands and their cross-sectional area, by dividing (9) by (10):

$$k_\ell = \frac{\frac{P_{e,j}}{n_j A_{s,j}^2}}{P_{r,j} n_j A_{s,j}}. \quad (11)$$

This can be restated as

$$k_\ell = \frac{\overline{\left[\begin{array}{cc} \frac{di_1}{dt} & \frac{di_2}{dt} \end{array}\right] \tilde{\mathbf{D}}_j \left[\begin{array}{c} \frac{di_1}{dt} \\ \frac{di_2}{dt} \end{array}\right]}}{I_{rms,j}^2 \ell_{w,j} \rho_c}. \quad (12)$$

### *B. Cost/Loss Optimization*

With a value of $k_\ell$ calculated, the analysis in [11], [12] can be applied almost directly to optimize cost and loss. The analysis assumes that the cost of litz wire can be approximately described by

$$Cost = (C_0 + C_m(d_c) d_c^2 n)\ell \quad (13)$$

where $C_0$ is a base cost per unit length associated with the bundling and serving operations, $C_m(d_c)$ is a cost basis function proportional to the additional cost per unit mass for a given strand diameter $d_c$, $n$ is the number of strands, and $\ell$ is the length of the wire. For the purpose of optimization with a fixed winding length, we can ignore $C_0$, and consider only the cost variation which is proportional to $C_m(d_c) d_c^2 n$. In [11], [12], a curve fit to manufacturers' data finds a function that can be used to approximate $C_m(d_c)$

$$C_m(d_c) = 1 + \frac{k_1}{d_c^6} + \frac{k_2}{d_c^2} \quad (14)$$

where $d_c$ is in meters, $k_1 = 1.1 \times 10^{-26}$ m$^6$, $k_2 = 2 \times 10^{-9}$ m$^2$, and $C_m(d_c)$ is normalized to a value of one for large $d_c$.

A solution for the minimum cost at any loss and vice versa is found in [11], [12]. The solution assumes (13) but, because it can be expressed in terms of $C_m(d_c)$, is valid either for the particular cost function given in (14), or for any other $C_m(d_c)$ that might be substituted to represent cost for a particular manufacturer or cost reduced by a new manufacturing technology. One convenient way to express the result is in terms of the optimum eddy current loss factor $F_e$,

$$F_{e,CL}(d_c) = 1 + \frac{1}{1 - \frac{2C_m(d_c)}{C_m'(d_c) d_c}} \quad (15)$$

For the particular cost function given in (14), the result is plotted in Fig. 2 and listed in Table III. This solution is valid if the available space in the bobbin window does not preclude the design implicitly specified by (15). Where window space becomes a more important constraint, the detailed analysis of area tradeoffs in litz wire discussed in [3] would become important.

Given an optimal value of $F_e$ for a given strand size, $F_{e,CL}$, the number of strands can be found from (4), and then the cost can be found from (13) and the total winding loss can be found from eddy loss (9) summed with resistive loss (10). If these calculations are repeated for a range of different strand sizes,

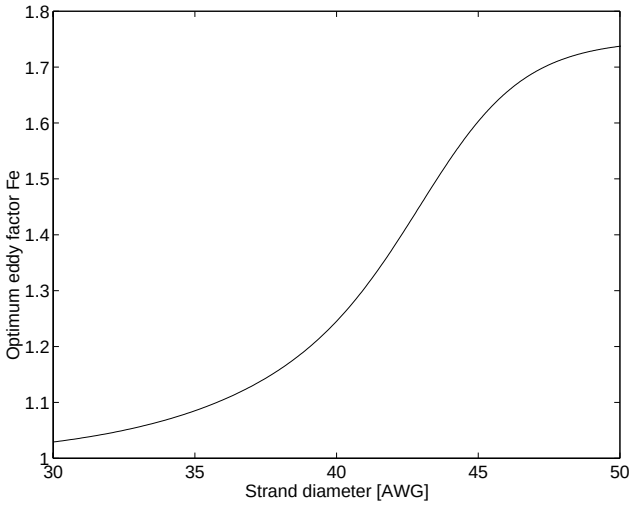


Fig. 2. Eddy loss factor, $F_e$, for optimal cost/loss tradeoff designs as a function of strand diameter. These data are valid for any geometry or frequency, given the cost function modeled by (14).

TABLE III
PARAMETERS FOUND FOR OPTIMAL COST/LOSS DESIGNS USING STANDARD STRAND SIZES, GIVEN THE COST FUNCTION MODELED BY (14).

| Strand gauge (AWG) | Relative cost | Relative loss | $F_e$ for optimal cost/loss tradeoff |
|---|---|---|---|
| 32 | 0.031 | 9.4 | 1.045 |
| 34 | 0.049 | 6.22 | 1.068 |
| 36 | 0.079 | 4.14 | 1.104 |
| 38 | 0.131 | 2.80 | 1.161 |
| 40 | 0.234 | 1.90 | 1.246 |
| 42 | 0.45 | 1.35 | 1.376 |
| 44 | 1 | 1 | 1.535 |
| 46 | 2.83 | 0.77 | 1.655 |
| 48 | 10.5 | 0.61 | 1.715 |
| 50 | 46 | 0.48 | 1.737 |

a menu of choices optimized for different cost/loss tradeoffs will result. The preferred design can be selected from these options based on the relative importance of cost and loss in the application, or based on a valuation of the loss [12].

It is observed in [11], [12] that these calculations result in identical curves of cost vs. loss for any design, if the results are normalized to the values for the same wire size. Such a curve, normalized to the 44 AWG results, is shown in Fig. 3, again based on the particular cost function given in (14). Using this curve, one need only calculate the cost and loss of one optimum design (e.g., AWG 44) in order to find the scale factors for the axes of Fig. 3, and then select from the choices it displays. The corresponding data is also listed in Table III. A flow chart for such a design procedure is given in [11], [12].

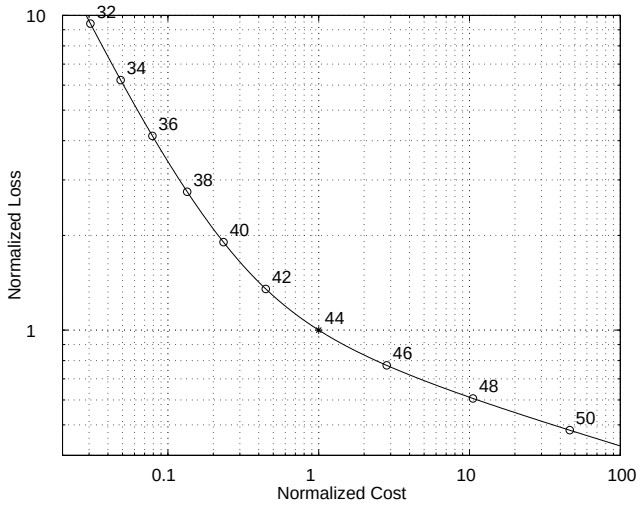


Fig. 3. Cost and loss, normalized to an optimal cost/loss design using 44 AWG strands. This graph applies to any design in which the bobbin is not full, given the cost function (14). Points are indexed with the AWG strand size used. Note that a point on this graph does not represent the minimum-loss design for that strand gauge; rather, it represents the minimum-loss design at a given cost; the strand size used to achieve this is indicated.

### C. Software Implementation of Calculations

The calculations described above have been implemented in the MATLAB language, in a program capable of handling any number of windings. A user interface is currently being developed for this program.

## IV. APPLICATION TO FLYBACK TRANSFORMER

The method described in Section III has been applied to the transformer described in Table I. The result is a range of possible designs as listed in Table IV, each with a different tradeoff between loss and cost, but often with substantial reductions in both. One higher-cost design that theoretically cuts the loss by more than half is also listed.

The designs listed all use the same strand size in both primary and secondary winding, but use different numbers of strands in each. This is ordinarily the optimum solution, because it places both windings on points of the same slope on Fig. 3. For example, in a two winding transformer with similar-size windings, if one winding used 48 AWG wire and the other used 40 AWG wire, changing both to 44 AWG wire would cut the total cost and cut the total loss, as can be seen from the slopes in Fig. 3. This assumes that the winding height is limited by cost and eddy loss, not by a full bobbin. If one winding had mostly low-frequency or dc current, and had no ac field induced by the other windings, the size of that low-frequency winding would be determined by the available bobbin space, not by the considerations discussed here. A good design procedure is to start by analyzing the optimum cost/loss designs as described here, with the same diameter of strands in each winding, and to mismatch strand sizes only if some of the designs produced do not fit on the bobbin.

Prototypes of each of these designs were constructed and tested in the flyback converter. Because the improved designs call for using a smaller volume of wire, space is gained, allowing some freedom in how the windings are placed in the window. If the windings remain immediately adjacent, their lower height leads to lower leakage inductance. This is advantageous for the circuit, but it also leads to higher $di/dt$ in the winding and thus to higher eddy-current losses. In this work we wish, for the moment, to avoid consideration of tradeoffs between losses in different parts of the circuit. Instead, we wish to leave the circuit operation unchanged. With the windings spaced apart slightly, it is possible to keep the leakage inductance close to that of the original design, satisfying the original goal of not modifying the circuit behavior and only decreasing the loss in the winding. Most of the prototype transformers were constructed to achieve near the original leakage inductance. To confirm the effect of leakage inductance, we also constructed some transformers with the windings closer together or further apart. For design B, all three possibilities were tested, and are listed in Table V as B1, B2 and B3.

The performance of the prototypes was measured in the cir-

TABLE IV
POSSIBLE DESIGNS AS CALCULATED

| Design | Strand Gauge [AWG] | Strand Diameter [mm] | Number of Strands | | Relative Wire Cost Estimate | Loss [W] |
|---|---|---|---|---|---|---|
| | | | Primary | Secondary | | |
| A (orig.) | 38 | 0.1 | 100 | 28 | 100% | 0.72 |
| B | 40 | 0.08 | 84 | 14 | 43% | 0.64 |
| C | 42 | 0.063 | 210 | 36 | 83% | 0.45 |
| D | 44 | 0.05 | 500 | 85 | 185% | 0.34 |

TABLE V
EXPERIMENTAL MEASUREMENTS WITH NEW DESIGNS

| Design | Leakage Inductance | Temperature Rise [°C] | | Estimated loss [W] | | |
|---|---|---|---|---|---|---|
| | | winding | core | copper | core | total |
| A | 0.26 $\mu$H | 37.7 | 23 | 1.02 | 0.39 | 1.41 |
| B1 | 0.18 $\mu$H | 46.6 | 25.9 | 1.15 | 0.37 | 1.52 |
| B2 | 0.25 $\mu$H | 38.7 | 20.8 | 0.85 | 0.41 | 1.26 |
| B3 | 0.39 $\mu$H | 49 | 28.2 | 1.24 | 0.36 | 1.6 |
| C | 0.23 $\mu$H | 34.8 | 21 | 0.79 | 0.42 | 1.21 |
| D | 0.28 $\mu$H | 26 | 23.4 | 0.79 | 0.39 | 1.18 |

cuit, and with out-of-circuit sinusoidal ac-resistance measurements. Previous work has confirmed the validity of the SFD method in predicting ac-resistance measurements [4], so we focus here on the in-circuit results. Performance was evaluated by measuring in-circuit temperature rise, listed in Table V. Winding loss was estimated using measured temperature rise and thermal resistance (measured using dc excitation of the winding). The thermal model assumes that the winding temperature rise is determined by the total core and winding loss power flowing through this single thermal resistance. Note that, because of the different sizes of the windings, the thermal resistances for each design differ. This explains the different trends in the winding temperature rise and winding loss columns of Table V. Core loss was estimated not from temperature rise but from out-of-circuit measurements of core loss as a function of ac flux amplitude with sinusoidal ac waveforms. Any dc-bias effects on core loss were ignored.

The experimental results consistently show higher temperature rises than we would predict based on the predicted loss. However, the trends are as predicted, both in that the new, improved designs are confirmed to have both lower loss and lower temperature rise, and in that the low-leakage design has increased loss compared to an otherwise-equivalent design with the original leakage inductance. The experimentally confirmed advantages of the new designs can be summarized as follows: Design C cuts the loss by 20 to 40%, with similar or slightly decreased cost, compared to the original design. Design B2 has loss about the same or a little lower than that of the original design, but it is estimated to cut the wire cost in half. Design D exceeds the original cost, but is intended to cut winding loss to less than half that in the original design. It does in fact have low losses, but they may not be as low as predicted. It has the lowest temperature rise, 30% less than the original design, but the estimated reduction in winding loss is only 23%.

The experimental results confirm the utility of the new method for producing new designs that reduce loss without increased cost, or even with reduced cost. However, they leave open questions about why there is a discrepancy between the expected and actual temperature rise. Although the thermal model used was greatly simplified, attempts to account for the discrepancies using more complex thermal models of the transformer did not indicate any plausible possibilities. However, a more complex thermal model of the overall converter might explain higher-than-expected temperature rise in the transformer, if there was significant heat conduction from other lossy components, such as the power MOSFET, into the transformer. In the experimental prototype, the transformer was positioned apart from the the other lossy components in order to minimize this effect.

Another possible explanation for discrepancies between theoretical and measured loss is that ringing in the primary current waveform during the turn-off transition, not accounted for in our ideal triangular waveforms, increases the loss in the winding. For example, if the MOSFET is considered an ideal switch with some parallel capacitance, the leakage inductance will ring with the capacitance when the switch turns off until the energy originally stored in the leakage inductance is all dissipated in the winding resistance. The resulting loss would be on the order of 2 W, independent of winding resistance. Thus, even a small fraction of this energy being lost in the winding could account for much of the discrepancy. It would be possible to include a more detailed current waveform, including ringing, in the calculation of $k_\ell$ (12), but it is not, in fact, advantageous to do so, because the optimization would then falsely indicate that the winding resistance could affect

this loss, when in fact the loss in a ringing process depends only on the initial energy in the ring, not on the rate at which it is dissipated. Further measurements are needed in order to determine whether the magnitude of this ring energy is sufficient to explain the observed discrepancies. Another possible partial explanation is the difference in core losses between the sinusoidal, zero-bias test we used to estimate losses and the actual non-sinusoidal waveform [18] with dc bias [19], [20].

To summarize, we have not thoroughly evaluated all of the loss and thermal effects in this circuit. This leaves open some question as to the reason for the temperature rise we observe. Some of the energy stored in the leakage inductance, lost during the switch transition, may end up in the transformer, either through ringing dissipated in winding resistance or through thermal conduction. The experimental results, including a higher-than-expected temperature rise on the high-leakage design B3, are qualitatively consistent with these explanations. In any case, we have confirmed that the new winding designs do in fact reduce loss and temperature rise, often with reduced cost as well.

## V. Conclusion

This paper has addressed the development of a new litz-stranding optimization method and has addressed the optimization of a particular flyback transformer.

The new litz-stranding optimization method allows generating a curve of possible cost-loss tradeoffs that can be obtained by selecting the number and diameter of strands. The curve is identical in form to those discussed in [11], [12]. However, unlike [11], [12], which were restricted to simple geometries and identical current waveforms in each winding, we have used the SFD method [4] to extend the results to arbitrary waveforms and geometries. The utility and validity of the method were confirmed by reducing both cost and loss in the example of a flyback transformer.

In the flyback transformer we evaluated, the effect of the fringing field near the gap was found to be small, despite the high ripple current in this discontinuous-conduction design. Instead, the loss was dominated by the eddy currents induced by the rapid changes in the field when the current commutates from one winding to the other. Those losses were reduced by changing strand number and diameter, as calculated by the new method. The reduction of losses was experimentally confirmed, although the observed temperature rise has not been fully explained in the original or the improved transformers.

We did not consider modifications to the flyback transformer design that would affect the leakage inductance. All else equal, decreased leakage inductance decreases circuit loss, but increases transformer loss because of higher $di/dt$. Future work should consider these tradeoff while examining design changes such as interleaved windings that reduce leakage inductance. For any new winding configuration, the stranding optimization developed here will remain useful.

## References


[1] J.G. Breslin and W.G. Hurley, "Derivation of optimum winding thickness for duty cycle modulated current waveshapes", in *28th Annual IEEE Power Electronics Specialists Conference*, 1997, vol. 1, pp. 655–661.

[2] Charles R. Sullivan, "Optimal choice for number of strands in a litz-wire transformer winding", in *28th Annual IEEE Power Electronics Specialists Conference*, 1997, pp. 28–35.

[3] Charles R. Sullivan, "Optimal choice for number of strands in a litz-wire transformer winding", *IEEE Transactions on Power Electronics*, vol. 14, no. 2, pp. 283–291, 1999.

[4] Charles R. Sullivan, "Computationally efficient winding loss calculation with multiple windings, arbitrary waveforms, and two- or three-dimensional field geometry", *IEEE Transactions on Power Electronics*, vol. 16, no. 1, 2001.

[5] W.G. Hurley, E. Gath, and J.G. Breslin, "Optimizing the ac resistance of multilayer transformer windings with arbitrary current waveforms", *IEEE Transactions on Power Electronics*, vol. 15, no. 2, pp. 369–76, Mar. 2000.

[6] Rudy Severns, "Additional losses in high frequency magnetics due to non ideal field distributions", in *APEC '92. Seventh Annual IEEE Applied Power Electronics Conference*, 1992, pp. 333–8.

[7] Jiankun Hu and C. R. Sullivan, "The quasi-distributed gap technique for planar inductors: Design guidelines", in *Proceedings of the 1997 IEEE Industry Applications Society Annual Meeting*, 1997, pp. 1147–1152.

[8] Peter Wallmeier, N. Frohleke, and H. Grotstollen, "Improved analytical modeling of conductive losses in gapped high-frequency inductors", in *Proceedings of the 1998 IEEE Industry Applications Society Annual Meeting*, 1998, pp. 913–920.

[9] Jiankun Hu and Charles R. Sullivan, "Optimization of shapes for round-wire high-frequency gapped-inductor windings", in *Proceedings of the 1998 IEEE Industry Applications Society Annual Meeting*, 1998, pp. 900–906.

[10] Jiankun Hu and Charles R. Sullivan, "Analytical method for generalization of numerically optimized inductor winding shapes", in *30th Annual IEEE Power Electronics Specialists Conference*, 1999.

[11] Charles R. Sullivan, "Cost-constrained selection of strand wire and number in a litz-wire transformer winding", in *Proceedings of the 1998 IEEE Industry Applications Society Annual Meeting*, 1998, pp. 907–911.

[12] Charles R. Sullivan, "Cost-constrained selection of strand wire and number in a litz-wire transformer winding", *IEEE Transactions on Power Electronics*, 2001.

[13] J. H. Spreen, "Electrical terminal representation of conductor loss in transformers", *IEEE Transactions on Power Electronics*, vol. 5, no. 4, pp. 424–9, 1990.

[14] J. M. Lopera, M. J. Prieto, F. Nuno, A. M. Pernia, and J. Sebastian, "A quick way to determine the optimum layer size and their disposition in magnetic structures", in *28th Annual IEEE Power Electronics Specialists Conference*, 1997, pp. 1150–1156.

[15] R. Prieto, J. A. Cobos, O. Garcia, P. Alou, and J. Uceda, "High frequency resistance in flyback type transformers", in *Fifteenth Annual IEEE Applied Power Electronics Conference*, 2000, vol. 2, pp. 714–19.

[16] Charles R. Sullivan, "Winding loss calculation with multiple windings, arbitrary waveforms, and two-dimensional field geometry", in *Proceedings of the 1999 IEEE Industry Applications Society Annual Meeting*, 1999, pp. 2093–9.

[17] E. C. Snelling, *Soft Ferrites, Properties and Applications*, Butterworths, second edition, 1988.

[18] J. Reinert, A. Brockmeyer, and R.W. De Doncker, "Calculation of losses in ferro- and ferrimagnetic materials based on the modified steinmetz equation", in *Proceedings of 34th Annual Meeting of the IEEE Industry Applications Society*, 1999, pp. 2087–92 vol.3.

[19] Wai Keung Mo, D.K.W. Cheng, and Y.S. Lee, "Simple approximations of the dc flux influence on the core loss power electronic ferrites and their use in design of magnetic components", *IEEE Transactions on Industrial Electronics*, vol. 44, no. 6, pp. 788–99, 1997.

[20] A. Brockmeyer and J. Paulus-Neues, "Frequency dependence of the ferrite-loss increase caused by premagnetization", in *Twelfth Annual Applied Power Electronics Conference and Exposition*, 1997, pp. 375–80.